Title: Vegetative phase change in *Populus tremula x alba*.

Authors: Erica H. Lawrence[1*], Aaron R. Leichty[1,2], Cathleen Ma[3], Steven H. Strauss[3] and R. Scott Poethig[1]

[1]Department of Biology, University of Pennsylvania, Philadelphia, Pennsylvania, 19104 USA
[2]Department of Plant Biology, University of California, Davis, California, 95616 USA
[3]Department of Forest Ecosystems and Society, Oregon State University, Corvallis, Oregon 97331
*Corresponding author: lawrence.erica.h@gmail.com

Key Words: Development, Juvenile-to-Adult Transition, miR156, *Populus* (Poplar), Vegetative Phase Change

Summary

- Plants transition through juvenile and adult phases of vegetative development in a process known as vegetative phase change (VPC). In poplars (genus *Populus*) the differences between these stages are subtle, making it difficult to determine when this transition occurs. Previous studies of VPC in poplars have relied on plants propagated *in vitro,* so the normal nature of this process is still unknown.

- We examined developmental morphology of seed-grown and *in vitro* derived *Populus tremula x alba* (clone 717-1B4), and compared the phenotype of these, to plants over- and under-expressing miR156, the master regulator of VPC.

- In seed-grown plants, most traits changed from node-to-node during the first 3 months of development but remained relatively constant starting around node 25. Most of these traits remained unchanged in clones over-expressing miR156, demonstrating they are regulated by the miR156/SPL pathway. Leaf fluttering--a characteristic of *Populus tremula* ("quaking aspen")--is one of these miR156-regulated traits.

- Vegetative development in plants grown from culture mirrored that of seed-grown plants, allowing direct comparison between plants often used in research and those found in nature. These results provide a foundation for further research on the role of VPC in the ecology and evolution of this economically important genus.

Introduction

During their ontogeny, plants transition through distinct phases, which is reflected in morphological variation in the organs produced at different times in development. These developmental transitions include the visually obvious transition between vegetative and reproductive growth as well as the often more subtle change between juvenile and adult vegetative stages, known as vegetative phase change (Ashby, 1948; Brink, 1962; Doorenbos, 1965; Poethig, 2013). In species with abrupt changes in vegetative morphology—termed *heteroblastic*—the distinction between the juvenile and adult phases is unambiguous (Zotz *et al.*, 2011). For example, many species of *Acacia* transition from producing bipinnate compound leaves to producing a simple undivided leaf termed a phyllode (Walters & Bartholomew, 1984). Other examples include *Eucalyptus globulus*, which transitions from producing ovate, wax-covered leaves to producing lanceolate glaucous leaves (James & Bell, 2001) and *Ipomoea caerulea,* which transitions from producing monolobed to trilobed leaves (Ashby, 1948). The juvenile-to-adult transition is more difficult to identify in species that experience less drastic changes in leaf and shoot morphology, with the result that we know very little about the duration of these phases in different taxa, or the relationship between this developmental transition and other aspects of plant life history, such as the response of plants to various biotic and abiotic conditions. However, even in these so-called *homoblastic* species (Goebel, 1900), organs produced early in shoot development differ from organs produced later in shoot development in a variety of morphological, anatomical, and physiological traits (Feng *et al.*, 2016). Identifying these traits and determining which are components of vegetative phase change and which are regulated by other factors, such as plant size or chronological age, is an important problem in plant development.

In *Arabidopsis* and most other plants, the transition from the juvenile to the adult phase of vegetative development is regulated by the closely related microRNAs, miR156 and miR157 (Poethig, 2013; He *et al.*, 2018). These miRNAs directly repress members of the Squamosa

62 Promoter Binding Protein-Like (SPL) family of transcription factors (Rhoades *et al.*, 2002;
63 Schwab *et al.*, 2005) which promote adult traits (Xu *et al.*, 2016). SPL expression is inhibited
64 during the juvenile phase by high levels of miR156/miR157. As plants age, miR156/miR157
65 expression declines, allowing for the increased expression of their SPL targets. This coordinated
66 change in miR156 and SPL gene expression leads to the onset of adult traits, with different traits
67 typically appearing at slightly different times in shoot development, depending on their
68 sensitivity to the level of SPL proteins (He *et al.*, 2018).
69 Vegetative phase change is a particularly important in long-lived perennial species, such
70 as trees, because the ability of these species to survive long enough to become reproductively
71 competent depends on their ability to respond to changing conditions over a long period of time.
72 Poplars are of considerable economic and ecological importance and have become popular
73 model systems for tree biology because they can be readily propagated in culture and are
74 susceptible to *Agrobacterium*-mediated transformation (Taylor, 2002). Temporal variation in leaf
75 and shoot morphology, and the phenotype of plants over-expressing miR156, have been
76 described in clones of *Populus x canendensis* (Wang *et al.*, 2011) and *P. tremula x alba*
77 (Rubinelli *et al.*, 2013). However, the significance of this information for vegetative phase
78 change in *Populus* is still unknown because the developmental morphology of seed-grown plants
79 has never been described. Here, we compare the vegetative phenotype of seed-grown *Populus*
80 *tremula x alba* with plants originating from explants in tissue culture and identify phase-specific
81 traits by characterizing the phenotype of plants over- and under-expressing miR156. We found
82 that shoot development in plants propagated *in vitro* closely resembles the development of seed-
83 grown plants, and that vegetative phase change occurs very early in both types of shoots. Most of
84 the traits we examined changed significantly as the shoot developed, and most of these traits
85 were sensitive to the level of miR156. One of these was leaf fluttering, a trait that has a
86 significant effect on photosynthetic efficiency (Roden & Pearcy, 1993b). Our results provide
87 basic information about the nature of vegetative phase change in *Populus tremula x alba and*
88 demonstrate that shoots regenerated *in vitro* can be used as models of primary shoot development
89 in this species.
90
91 **Materials and Methods**
92 *Plant transformation*

93 Assembly of Ubi10:AthMIR156a and Ubi10:MIM156 constructs have previously been
94 described (Feng *et al.*, 2016). Additionally, a second MIM156 construct was designed using
95 Golden Gate Cloning (Engler *et al.*, 2014). Further details of construct assembly can be found in
96 Table S1.
97 Poplar line 717-1B4 was transformed using *Agrobacterium tumefaciences (strain AGL1)*
98 following the protocol described in Filichkin *et al.* (2006). Briefly, leaf and stem explants were
99 selected on callus-induction, shoot induction, shoot elongation and rooting media using BASTA.
100 A total of 30 Ubi:AthMIR156a events and 25 Ubi:MIM156 events were isolated. Of these, two
101 lines for each construct type were selected based on levels of miR156 in 5 cm leaf primordia
102 (data not shown). For the Ubi:AthMIR156a and Ubi:MIM156 constructs made with the pCambia
103 3300 backbone, the Ubi:AthMIR156a construct had a higher rate of producing transgenic shoots
104 (percent of explants forming shoots was 52% versus 33.9%). We did not track efficiency for the
105 other MIM156 construct.
106
107 *Plant material and growth conditions*
108 *Populus tremula x alba* line 717-1B4, two independent miR156 over-expressor lines, 40
109 and 78, and two independent MIM156 lines, 22 and 84, were obtained by *in vitro* propagation
110 and hardening on propagation media as described in Meilan and Ma (2006). Plants were then
111 transplanted to Fafard-2 growing mix (Sungro Horticulture, Massachusetts, USA) in 0.3-L pots
112 in the greenhouse at the University of Pennsylvania (39.9493°N, 75.1995°W, 22.38 m a.s.l.) and
113 kept in plastic bags for increased humidity for 2 weeks. Plants were transferred to 4.2-L pots
114 with Fafard-52 growing mix 3 weeks later and fertilized with Osmocote 14-14-14 (The Scotts
115 Company, Marysville, OH, USA), supplemented by weekly applications of Peters 20-10-20 (ICL
116 Fertilizers, Dublin, OH, USA). Plants were grown at a temperature ranging from 22 and 27°C on
117 a 16 hr photoperiod, with illumination provided by a combination of natural light and 400-W
118 metal halide lamps (P.L. Light Systems, Ontario, Canada) with daily irradiances between 300
119 and 1,500 μmol m^{-2} s^{-1}. Planting of individuals was staggered across three months with the
120 position of plants in the greenhouse randomized and individuals rotated frequently.
121 *Populus tremula x alba* seeds were purchased from Sheffield's Seed Company (Locke,
122 NY), and were germinated on a layer of vermiculite on top of Fafard-2 growing mix in 0.64-L
123 pots in the greenhouse under conditions described above. Seedlings were transplanted one month

124 after germination into Fafard-52 growing mix in 1.76-L pots, fertilized with Osmocote 14-14-14.
125 They were transplanted to 4.2-L pots 3 months later. Planting of individuals was staggered across
126 five months and individuals were rotated within the greenhouse frequently.
127
128 *Mir156/7 expression*
129 The abundance of miR156 and miR157 RNA was measured in <1 cm leaf primordia.
130 Total RNA was isolated using the Spectrum^{TM} Plant Total RNA Kit (Sigma-Aldrich), according
131 to the manufacturer's instructions. RNA levels were measured by RT-qPCR, using primers
132 specific for miR156, miR157 and miR159 in combination with the stem-loop RT primers
133 described in Varkonyi-Gasic et al. (2007) (Table S2). miR159 was used as an endogenous
134 control (Leichty & Poethig, 2019) and validated across all time points in seed-grown plants.
135 cDNA was synthesized using Invitrogen SuperScript III following the methods of Varkonyi-
136 Gasic et al. (2007). Platinum Taq (Invitrogen) was used with the Roche universal hydrolysis
137 probe #21, and a three-step amplification protocol. Relative measures of abundance were
138 calculated using the $2^{-\Delta\Delta Ct}$ method (Livak & Schmittgen, 2001).
139
140 *Stomatal impressions, epidermal traits, petiole morphology and abaxial trichome density.*
141 Stomatal density and epidermal cell size were measured using clear nail polish
142 impressions of adaxial and abaxial surfaces. Trichomes were removed from the abaxial side of
143 leaves with tape when necessary, and three sections per leaf were imaged and photographed
144 using an Olympus BX51 light microscope. Hand sections of leaf petioles within 1 cm of leaf
145 attachment site were imaged as described above. Trichome density on the abaxial side of the leaf
146 was measured using an Olympus MVX10 dissecting scope. Measurements were made along the
147 mid vein, where the density was low enough to permit accurate counts. All measurements and
148 counts were made using Fiji software.
149
150 *Leaf vein densities*
151 Sections from fully expanded leaves were cleared using NaOH and bleach, and then
152 stained with Safranin following the protocol described in Scoffoni and Sack (2013). Vein lengths
153 of all visible vein orders were measured from microscope images using Fiji software, and vein
154 densities were calculated following Scoffoni and Sack (2013).

155

156 *Leaf shape and size*

157 Fully expanded leaves were attached to paper using double-sided tape and scanned. The
158 scanned images were measured using the Morphological Analysis of Size and Shape (MASS)
159 software (Chuanromanee *et al.*, 2019).

160

161 *Leaf initiation rate, internode distance and branching*

162 The leaf initiation rate was determined by counting the node of the uppermost visible leaf
163 at least twice a week. The number of branches at least 1 cm in length between nodes 1 and 25
164 was determined after 230 days of growth.

165

166 *Fluttering*

167 To measure leaf fluttering, plants were placed 100 cm away from a fan, with the leaf to
168 be measured facing perpendicular to the wind. Wind speeds at the sample leaf position were 1.5
169 m/s as measured with an anemometer. Leaf movement was filmed at 240 fps for 30 seconds
170 (representative example in supplemental file "Poplar Fluttering Video"). Leaf movement was
171 analyzed by following the movement of a mark placed at the tip of the leaf using Tracker video
172 analysis and modeling tool v5.0.7. The height and width of the petiole were measured using a
173 digital caliper.

174

175 *Statistical Analysis*

176 All statistical analyses were performed in JMP® Pro v. 14.0.0 (SAS Institute Inc., Cary,
177 NC). Traits in seed grown poplar across leaf positions were measured from a minimum of 42
178 individuals and fit with a linear or second-degree polynomial as appropriate with p-values and R^2
179 values reported. Traits that were examined at multiple leaf positions in 717 wildtype, MIM156
180 lines 84 and 22 and miR156 over-expression lines 40 and 78 were measured from a minimum of
181 6 individuals and compared by two-way *ANOVA* and a Student's t test ($\alpha = 0.05$) where leaf
182 position and genotype were the main effects. Whole-plant measures of branching and internode
183 length in these plants was compared by one-way *ANOVA* where genotype was the main effect
184 and a Student's t test ($\alpha = 0.05$), and leaf emergence was compared by two-way *ANOVA* with
185 days after transplant and genotype as the main effects.

186

187 **Results**

188 *miR156/7 expression in seed grown plants and 717-1B4 lines*

189 The miR156/7 expression pattern in the leaf primordia of seed-grown plants matched that
190 previously reported for other species, such as *A. thaliana* and *Vachellia* sp. (He *et al.*, 2018;
191 Leichty & Poethig, 2019). miR156/7 abundance dropped 7-fold between nodes 1 and 10,
192 followed by a slower decline in successive nodes (Fig. **1A**). We first determined that the control
193 small RNA, miR159, was expressed at the same level in leaves 15 and 25 of seed-grown plants
194 and the clone 717-1B4, and then measured the level of miR156/7 in wild-type and transgenic
195 genotypes of 717-1B4. The abundance of miR156/7 in the primordia of leaf 15 and 25 in
196 wildtype 717-1B4 was similar to the amount of miR156/7 in these same leaves in seed-grown
197 poplar (Fig. **1A, B**), suggesting that miR156/7 are expressed at comparable levels at the same
198 node in plants propagated by these methods. Leaf 15 and 25 of the miR156 over-expressor lines
199 had, respectively 4.9 and 5.6 times the amount of miR156a as wild-type leaves, a level
200 comparable to that of leaf 3 and 5 of seed-grown plants (Fig. **1A, B**). Although the amount of
201 miR156/7 in leaves 15 and 25 of the MIM156 lines was similar to that in 717-1B4 and seed-
202 grown poplar (Fig. **1A, B**), line 84 had approximately 1/3 the amount of miR156 at an earlier
203 stage of development, before it was transferred to soil (data not shown). Target mimics do not
204 necessarily reduce the level of their target miRNAs (Franco-Zorrilla *et al.*, 2007), so the
205 significance of these MIM156 data is difficult to interpret. In any case, the similarity between the
206 amount of miR156/7 in MIM156 and wild-type lines shows that the transformation protocol and
207 vector components have no independent effect on miR156/7 abundance.

208

209 *Changes in miR156 expression alter plant growth rate and form*

210 Plants grown from seed produced leaves at a relatively slow rate for the first few weeks
211 after planting, and transitioned to a faster, linear growth rate after producing 15-20 leaves (Fig.
212 **3A**). Leaf initiation in wild-type and transgenic clones of 717-1B4 was delayed for 35-40 days
213 after transplanting to soil, and then occurred at increasing rate over the next 2-3 weeks of
214 measurement. During this latter period, lines transformed with Ubi10:AthMIR156a had higher
215 rates of leaf initiation than either wild-type or MIM156 lines (Fig. **3B**). Ubi10:AthMIR156a lines
216 also had shorter internodes than either the wild-type and MIM156 lines (Fig. **3C**) and produced

217 significantly more axillary branches than these genotypes (Fig. **3D**). The MIM156 lines were not
218 significantly different from 717-1B4 for any of these traits, although these lines did have slightly
219 longer internodes than 717-1B4.
220
221 *Juvenile and adult leaves differ in leaf shape and size*
222 The leaves of seed-grown plants became gradually rounder (decreased L:W ratio) (Fig.
223 **4A**) and larger (Fig. **4C**) from node 1 to node 25 and did not change significantly in shape or size
224 after this point (Fig. **1C**). 717-1B4 displayed a similar trend, although the leaves of this clone
225 reached their climax shape and size a few nodes earlier than seed-grown plants (Fig. **2** and **4B,**
226 **D**). MIM156 lines did not differ significantly in size from 717-1B4, but the leaves of line 84
227 were rounder than 717-1B4 beginning at node 15. In contrast, the leaves of lines over-expressing
228 miR156 were significantly more elongated and smaller than wild-type leaves starting from node
229 15 (Student's *t* test $p < 0.05$). These results suggest that changes in leaf shape and size during
230 shoot development in poplar are partly regulated by a decrease in level of miR156.
231 To obtain a comprehensive picture of the effect of miR156 on leaf morphology in
232 *Populus tremula x alba*, we also measured the abaxial trichome density, stomatal density,
233 epidermal cell area, specific leaf area, vein density, and petiole morphology of successive leaves.
234 We examined every 5th leaf of seed-grown plants from germination to node 45-50, and every 5th
235 leaf of 717-1B4 and transgenic lines from node 10 to 25.
236 The leaves of *Populus alba* appear white because of a dense layer of trichomes on the
237 abaxial surface of the leaf blade, and this trait is also characteristic of *P. tremula x alba.* All the
238 leaves of *P. tremula x P. alba* produced abaxial trichomes, but trichome density increased
239 dramatically during shoot growth (Fig. **4G, H**). In seed-grown plants, abaxial trichome density
240 increased more than 10-fold between leaf 5 and leaf 40 and increased by about 6-fold between
241 leaf 10 and leaf 25 in 717-1B4. In contrast, abaxial trichome density remained at the same
242 relatively low level from node 10 to node 25 in the miR156 over-expressors, and it increased
243 significantly more than 717-1B4 in both MIM156 lines (Student's *t* test; $p < 0.01$ and $p < 0.0001$
244 for line 22 and 84 respectively). This result suggests that abaxial trichome production is a phase-
245 specific trait in *P. tremula x alba* and is hypersensitive to the level of miR156.
246 One factor that could contribute to this increase in trichome density is a decrease in
247 epidermal cell size, which would increase the number of epidermal cells per unit area. We

248 measured this trait by taking impressions of the adaxial epidermis, because the high density of
249 trichomes made it impractical to measure epidermal cell area on the abaxial surface. In seed-
250 grown plants, cell area decreased approximately 4-fold over the first 30 leaves and remained
251 relatively constant after this point (Fig. **4M**). In 717-1B4, cell area decreased about 2-fold from
252 leaf 10 to leaf 20, and decreased much less dramatically, if at all, between leaf 20 and leaf 25.
253 The MIM156 lines were not significantly different from 717-1B4. In contrast, cell area in the
254 miR156 over-expressors did not change significantly between leaf 10 and leaf 25. These results
255 suggest that epidermal cell area is a phase-specific trait, and also suggest that the increase in
256 abaxial trichome density is partly attributable to an increase in the cell density in the epidermis.
257 This is not the only explanation for the increase in abaxial trichome density, however, because
258 the magnitude of the change in trichome density and cell area is different, and because the
259 MIM156 had a significant effect on trichome density, but not cell area.
260 Stomatal density on both the adaxial and abaxial side of the leaf changed across leaf
261 positions, but in opposite directions (Fig. **4I, K**). In seed-grown plants, adaxial stomatal density
262 decreased linearly from leaf 5 to leaf 40, whereas abaxial stomatal density increased linearly
263 over this interval; at every node, the density of stomata on the adaxial surface of the leaf was
264 significantly less than that on the abaxial surface. Both 717-1B4 and the MIM156 lines had a
265 very low density of adaxial stomata on leaf 10, and this number was reduced to nearly zero on
266 leaf 25. In contrast, the density of abaxial trichomes in these genotypes increased significantly
267 between leaf 10 and leaf 25. In the miR156 over-expressing lines, the density of stomata on both
268 the adaxial and abaxial surfaces of leaves 10 and 25 was essentially identical to that of the basal-
269 most leaves of seed-grown plants. Thus, miR156 regulates stomatal density on both sides of the
270 leaf. However, other factors also contribute to the developmental changes in stomatal density
271 because this parameter changes linearly during shoot development, rather than in the curvilinear
272 pattern characteristic of the change in miR156 levels (Fig. **4J, L**).
273 Specific leaf area (SLA), is the area of the leaf blade per unit mass, and is determined by
274 the thickness of the leaf blade and cell density. SLA decreased in a curvilinear fashion from leaf
275 5 to leaf 40 in seed-grown plants and decreased linearly from leaf 10 to leaf 25 in 717-1B4 and
276 the 4 transgenic lines (Figure **4E, F**). However, SLA decreased nearly linearly between leaf 10
277 and leaf 25 in seed-grown plants, so these data do not reveal if there is a significant difference in
278 the pattern in seed-grown and clonally propagated plants. On the other hand, we found that—at

279 nodes 15-25—lines over-expressing miR156 had a significantly higher SLA, and one MIM156
280 line (84) had a significantly lower SLA, than 717-1B4 at node 10 (Student's *t* test, $p < 0.05$ and p
281 < 0.0001 for miR156 over-expressors at nodes 15 and 20, and node 25 respectively and $p = 0.019$
282 for line 84 node 10). These results suggest that SLA is a phase-specific trait and is regulated by
283 miR156.
284
285 *Leaf vein density increases as plants transition from juvenile to adult*
286 Leaf vein density increased 1.8-fold with increasing leaf position in 717-1B4 and in the
287 MIM156 lines, although MIM156 line 84 had a significantly higher vein density than 717-1B4 in
288 leaf 10 (Student's *t* test, $p < 0.01$). Similar results were obtained for the density of vein endings.
289 In the miR156 over-expressors, vein density and the density of vein endings did not differ much
290 between leaf 10 and leaf 25, and were identical to, or slightly lower than, the values observed for
291 leaf 10 in 717-1B4 (Fig. **5**).
292
293 *Petiole morphology changes during development leading to altered leaf fluttering behavior*
294 Many species of poplar, including *Populus tremula x alba,* exhibit leaf fluttering, a trait
295 that has been attributed to the vertical elongation of the petiole (Niklas, 1991). In a previous
296 study of *Populus x canadensis*, we found that the petioles of *in vitro* propagated plants became
297 increasing elongated as the shoot developed, and that over-expression of miR156 suppressed this
298 process (Wang et al. 2011). To determine if this phenomenon occurs naturally, we examined the
299 L:W ratio of a cross-section of the petiole in seed-grown *Populus tremula x alba* (Fig. **6A**). We
300 found that the petiole of leaves at node 10 was slightly broader than tall (L:W < 1), whereas the
301 petioles of leaves at higher nodes became vertically elongated (L:W >1), reaching their climax
302 shape around node 40. In wild-type 717-1B4, and in the MIM156 and miR156 over-expressors,
303 the petiole also became progressively elongated (Fig. **6B**). However, the miR156 over-expressors
304 had significantly less elongated petioles than the 717-1B4 and the MIM156 lines, and reached a
305 maximum L:W ratio at an earlier node. We also examined the effect of these transgenes on
306 petiole anatomy. In 717-1B4, the petioles of leaves at nodes 10 and 15 had an adaxial
307 indentation, a large central vascular bundle, and two smaller vascular bundles located in a
308 horizontal plane above the central bundle. The petioles of leaves 20 and 25 lacked an adaxial
309 indentation and had three vertically oriented vascular bundles that decreased in size from the

310 abaxial to the adaxial side of the petiole. In the MIM156 lines, the vascular anatomy of leaf 15
311 was intermediate between that of leaf 10 and leaf 20 in 717-1B4, indicating that the transition to
312 the adult shape is accelerated in these lines, despite the lack of a significant change in the L:W
313 ratio of the petiole (Fig. **6C**). Consistent with their L:W ratio, lines over-expressing miR156
314 retained a juvenile petiole morphology up to at least node 25. Petiole anatomy is therefore an
315 obvious qualitative indicator of the phase identity of a leaf in *Populus tremula x alba*.
316 To determine if this change in petiole morphology has an effect on the behavior of the
317 leaf, we looked at two measures of leaf fluttering—the total distance moved by the leaf, and the
318 maximum horizontal span of the leaf tip—when leaves were exposed to a constant wind velocity
319 (Fig. **7A**). There was a statistically significant (p <0.0001) positive linear relationship between
320 petiole L:W ratio and these fluttering measures in 717-1B4, the MIM156 and miR156 over-
321 expressing lines. Leaves at basal node 10 in the 717-1B4 and in the MIM156 lines fluttered less
322 than leaves at more apical node 25, whereas juvenile leaves at node 25 of the miR156 over-
323 expressing lines fluttered less than leaves at node 25 of the 717-1B4 and in the MIM156 lines
324 (Fig.**7B, C**). Thus, the petiole morphology of juvenile and adult leaves of *Populus tremula x alba*
325 has a significant effect on their response to wind.
326
327 **Discussion**
328 Many plants do not undergo visually abrupt changes in form during shoot development,
329 making the onset of vegetative phase change difficult to observe. As a result, the existence of this
330 phenomenon and its significance for plant ecology and evolution are often under appreciated. In
331 this study, we characterized the growth rate, developmental morphology, and temporal pattern of
332 miR156 expression in *Populus tremula x alba,* an ecologically and economically important tree.
333 We found that many leaf traits change during shoot development in plants grown from seeds, as
334 well as in shoots arising *de novo* in culture, and that most of these changes are correlated with
335 and sensitive to changes in the level of miR156. These data confirm and extend previous studies
336 of the effect of miR156 on *Populus* development (Wang *et al.*, 2011; Rubinelli *et al.*, 2013), and
337 provide a foundation for future research on the function of vegetative phase change in the life
338 history of this woody species.
339 In nature, poplars propagate primarily from adventitious shoots, whereas clones used for
340 research or commercial purposes are propagated from axillary buds or by inducing shoot

341 regeneration *in vitro* (Taylor, 2002). The extent to which these plants recapitulate the
342 development of the primary shoot is still unknown. We found by at least the 10th node, the
343 development of a regenerated shoot is remarkably similar to that of a seed-grown plant. This
344 result suggests that the phase-identity of poplar cells is either re-set during the de-differentiation
345 of the primary tissue sample, or during shoot regeneration. This observation also raises the long-
346 standing question of whether differentiated traits can be maintained in tissue culture.
347 Although vegetative phase change sometimes involves traits unique to a particular
348 species (Wang *et al.*, 2011; Leichty & Poethig, 2019), analyses of plants with altered levels of
349 miR156 have revealed a number of phase-specific traits that are common to phylogenetically
350 diverse species. In *Zea mays*, *Arabidopsis thaliana*, *Nicotiana tabacum,* and now *Populus*
351 *tremula x alba*, these traits include patterns of trichome production, leaf shape and size,
352 epidermal and stomatal cell traits, vein density, leaf initiation rate, and branching (Bongard-
353 Pierce *et al.*, 1996; Telfer *et al.*, 1997; Feng *et al.*, 2016; He *et al.*, 2018). At least some of these
354 traits are also regulated by miR156 in *Populus x canadensis* (Wang *et al.*, 2011), rice (Xie *et al.*,
355 2006), alfalfa (Aung *et al.*, 2015), switchgrass (Fu *et al.*, 2012), *Lotus japonicus* (Wang, 2014),
356 and tomato (Zhang *et al.*, 2011). This observation indicates that vegetative phase change is an
357 ancient and fundamental aspect of shoot development, and also suggests that the differential
358 expression of various traits during shoot development contributes to plant fitness and is therefore
359 under natural selection (Leichty & Poethig, 2019).
360 Determining how phase-specific traits contribute to plant fitness is challenging, however.
361 A number of studies have shown that plants over-expressing miR156 are more or less sensitive
362 to various environmental stresses (Stief *et al.*, 2014; Cui *et al.*, 2014; Arshad *et al.*, 2017; Kang
363 *et al.*, 2020), but there is still little evidence that juvenile and adult phases of wild type plants
364 display these same differences, or how they might contribute to plant fitness. There are relatively
365 few examples of phase-specific vegetative traits that are either known or expected to be
366 selectively advantageous (Williams *et al.*, 1998; Holeski *et al.*, 2009; Leichty & Poethig, 2019).
367 Our observation that adult leaves flutter more than juvenile leaves is another such example. In
368 poplar, leaf fluttering is beneficial under high light and high heat environments, but is
369 disadvantageous under low light conditions because it reduces photosynthesis (Roden & Pearcy,
370 1993a,b). This suggests that reduced leaf fluttering is advantageous early in development, when

371 plants are likely to be shaded by other plants, whereas increased fluttering is advantageous once
372 plants are no longer in the understory.
373 During shoot development, different morphological and physiological traits change in a
374 coordinated fashion, but not necessarily at the same node or at the same rate (Hackett & Murray,
375 1997; Leichty & Poethig, 2019). Furthermore, under certain conditions, traits can become
376 dissociated, resulting in leaves or shoots that have unusual combinations of juvenile and adult
377 traits (Robbins, 1960; Doorenbos, 1965). In our experiments, this was apparent from the
378 phenotype of transgenic lines expressing a miR156/miR157 target site mimic (MIM156). The
379 stronger of these transgenes had a significant effect on leaf L:W ratio, SLA, epidermal cell area,
380 petiole morphology and leaf vein density, but did not affect leaf initiation rate, stomatal density
381 and petiole L:W ratio. These observations are consistent with studies in in *Arabidopsis*, which
382 show that different miR156-regulated SPL genes have different transcription patterns and
383 sensitivity to miR156 abundance (Xu *et al.*, 2016; He *et al.*, 2018). Along with the evidence that
384 SPL genes also have different loss-of-function phenotypes (Xu *et al.*, 2016), these results suggest
385 that variability in the expression of different phase-specific traits may arise from the differential
386 response of functionally distinct SPL genes to changes in the level of miR156.
387 miR156 and its SPL targets control many economically important traits, including
388 flowering time, shoot architecture, biomass and lignin production, pest and disease resistance
389 and abiotic stress responses (Wang & Wang, 2015). In the biofuel crop *P. virgatum*, for example,
390 over-expressing miR156 leads to increases in biomass, digestibility, and lignin production, a
391 delay in flowering time, and altered susceptibility to the pathogen *Puccinia emaculata* (Chuck *et*
392 *al.*, 2011; Fu *et al.*, 2012; Baxter *et al.*, 2018). Similar effects of miR156 over-expression have
393 been observed in the forage legumes *Trifolium pretense* (Zheng *et al.*, 2016) and *Medicago*
394 *sativa* (Aung *et al.*, 2015). Poplars are fast-growing trees useful for a wide variety of industrial
395 purposes, as well for the re-forestation of degraded land (Taylor, 2002). The ability to engineer
396 their chemistry and vegetative development through the manipulation of miR156 offers new
397 opportunities for the improvement of this important group of plants.
398
399 **Acknowledgements**
400 We thank Samara Gray and Joshua Darfler for their assistance in caring for the plants used in
401 this study. This research was funded by the NSF Graduate Research Fellowship (DGE-1321851),

402 U. of Pennsylvania SAS Dissertation Research Fellowship and the Peachey Research Fund to
403 E.H.L., NIH T32GM008216 to A.R.L and NIH GM51893 to R.S.P.
404
405 **Author Contributions**
406 E.H.L., A.R.L., and R.S.P. planned and designed the research. E.H.L. and A.R.L. performed the
407 experiments. C.M., and S.H.S. helped create the transgenics used in this study. E.H.L performed
408 statistical analyses and wrote the first draft of the manuscript. E.H.L., A.R.L., C.M., S.H.S., and
409 R.S.P revised and provided comments on the manuscript.
410
411 **References**
412 **Arshad M, Feyissa BA, Amyot L, Aung B, Hannoufa A**. **2017**. MicroRNA156 improves
413 drought stress tolerance in alfalfa (Medicago sativa) by silencing SPL13. *Plant Science* **258**:
414 122–136.
415 **Ashby E**. **1948**. Studies in the morphogenesis of leaves. II. The area, cell size and cell number of
416 leaves of Ipomoea in relation to their position on the shoot. *New Phytologist* **47**: 177–195.
417 **Aung B, Gruber MY, Amyot L, Omari K, Bertrand A, Hannoufa A**. **2015**. Ectopic
418 expression of LjmiR156 delays flowering, enhances shoot branching, and improves forage
419 quality in alfalfa. *Plant Biotechnology Reports* **9**: 379–393.
420 **Baxter HL, Mazarei M, Dumitrache A, Natzke JM, Rodriguez M, Gou J, Fu C, Sykes RW,**
421 **Turner GB, Davis MF, *et al.* 2018**. Transgenic miR156 switchgrass in the field: growth,
422 recalcitrance and rust susceptibility. *Plant Biotechnology Journal* **16**: 39–49.
423 **Bongard-Pierce DK, Evans MMS, Poethig RS**. **1996**. Heteroblastic features of leaf anatomy in
424 maize and their genetic regulation. *International Journal of Plant Sciences* **157**: 331.
425 **Brink RA**. **1962**. Phase change in higher plants and somatic cell heredity. *The Quarterly Review*
426 *of Biology* **37**: 1–22.
427 **Chuanromanee TS, Cohen JI, Ryan GL**. **2019**. Morphological Analysis of Size and Shape
428 (MASS): An integrative software program for morphometric analyses of leaves. *Applications in*
429 *Plant Sciences* **7**: e11288.
430 **Chuck GS, Tobias C, Sun L, Kraemer F, Li C, Dibble D, Arora R, Bragg JN, Vogel JP,**
431 **Singh S, *et al.* 2011**. Overexpression of the maize Corngrass1 microRNA prevents flowering,
432 improves digestibility, and increases starch content of switchgrass. *Proceedings of the National*

433 *Academy of Sciences* **109**: 995–995.
434 **Cui L-G, Shan J-X, Shi M, Gao J-P, Lin H-X**. **2014**. The miR156-SPL9-DFR pathway
435 coordinates the relationship between development and abiotic stress tolerance in plants. *The*
436 *Plant Journal* **80**: 1108–1117.
437 **Doorenbos J**. **1965**. Juvenile and adult phases in woody plants. *Encyl. Plant Physiol.* **15**: 1222–
438 35.
439 **Engler C, Youles M, Gruetzner R, Ehnert T-M, Werner S, Jones JDG, Patron NJ,**
440 **Marillonnet S**. **2014**. A Golden Gate modular cloning toolbox for plants. *ACS Synthetic Biology*
441 **3**: 839–843.
442 **Feng S, Xu Y, Guo C, Zheng J, Zhou B, Zhang Y, Ding Y, Zhang L, Zhu Z, Wang H, *et al.***
443 **2016**. Modulation of miR156 to identify traits associated with vegetative phase change in
444 tobacco (Nicotiana tabacum). *Journal of Experimental Botany* **67**: 1493–1504.
445 **Filichkin SA, Meilan R, Busov VB, Ma C, Brunner AM, Strauss SH**. **2006**. Alcohol-
446 inducible gene expression in transgenic Populus. *Plant Cell Reports* **25**: 660–667.
447 **Franco-Zorrilla JM, Valli A, Todesco M, Mateos I, Puga MI, Rubio-Somoza I, Leyva A,**
448 **Weigel D, García JA, Paz-Ares J, *et al.* 2007**. Target mimicry provides a new mechanism for
449 regulation of microRNA activity. *Nature Genetics* **39**: 1033–1037.
450 **Fu C, Sunkar R, Zhou C, Shen H, Zhang J-YY, Matts J, Wolf J, Mann DGJ, Stewart CN,**
451 **Tang Y, *et al.* 2012**. Overexpression of miR156 in switchgrass (Panicum virgatum L.) results in
452 various morphological alterations and leads to improved biomass production. *Plant*
453 *Biotechnology Journal* **10**: 443–452.
454 **Goebel K**. **1900**. *Organography of Plants Part I. General Organography. (English Translation*
455 *by I. B. Balfour)*. Oxford: Clarendon Press.
456 **Hackett WP, Murray JR**. **1997**. Approaches to understanding maturation or phase change. In:
457 Geneve RL, Preece JE, Merkle SA, eds. Biotechnology of Ornamental Plants. New York: CAB
458 International, 73–86.
459 **He J, Xu M, Willmann MR, McCormick K, Hu T, Yang L, Starker CG, Voytas DF, Meyers**
460 **BC, Poethig RS**. **2018**. Threshold-dependent repression of SPL gene expression by
461 miR156/miR157 controls vegetative phase change in Arabidopsis thaliana. *PLOS Genetics* **14**:
462 e1007337.
463 **Holeski LM, Kearsley MJC, Whitham TG**. **2009**. Separating ontogenetic and environmental

464 determination of resistance to herbivory in cottonwood. *Ecology* **90**: 2969–2973.
465 **James SA, Bell DT**. **2001**. Leaf morphological and anatomical characteristics of heteroblastic
466 Eucalyptus globulus ssp. Globulus (Myrtaceae). *Australian Journal of Botany* **49**: 259–269.
467 **Kang T, Yu CY, Liu Y, Song WM, Bao Y, Guo XT, Li B, Zhang HX**. **2020**. Subtly
468 manipulated expression of ZmmiR156 in tobacco improves drought and salt tolerance without
469 changing the architecture of transgenic plants. *Frontiers in Plant Science* **10**: 1664.
470 **Leichty AR, Poethig RS**. **2019**. Development and evolution of age-dependent defenses in ant-
471 acacias. *Proceedings of the National Academy of Sciences* **116**: 15596–15601.
472 **Livak KJ, Schmittgen TD**. **2001**. Analysis of relative gene expression data using real-time
473 quantitative PCR and the 2-ΔΔCT method. *Methods* **25**: 402–408.
474 **Meilan R, Ma C**. **2006**. Poplar (Populus spp.). In: Wang K, ed. Methods in Molecular Biology:
475 Agrobacterium Protocols. Totowa, NJ: Humana Press Inc., 143–151.
476 **Niklas KJ**. **1991**. The elastic moduli and mechanics of Populus tremuloides (Salicaceae) petioles
477 in bending. *American Journal of Botany* **78**: 989–996.
478 **Poethig RS**. **2013**. Vegetative phase change and shoot maturation in plants. *Current Topics in*
479 *Developmental Biology* **105**: 125–152.
480 **Rhoades MW, Reinhart BJ, Lim LP, Burge CB, Bartel B, Bartel DP**. **2002**. Prediction of
481 plant microRNA targets. *Cell* **110**: 513–520.
482 **Robbins WJ**. **1960**. Further observations on juvenile and adult Hedera. *American Journal of*
483 *Botany* **47**: 485–491.
484 **Roden JS, Pearcy RW**. **1993a**. Effect of leaf flutter on the light environment of poplars.
485 *Oecologia* **93**: 201–207.
486 **Roden JS, Pearcy RW**. **1993b**. The effect of flutter on the temperature of poplar leaves and its
487 implications for carbon gain. *Plant, Cell and Environment* **16**: 571–577.
488 **Rubinelli PM, Chuck G, Li X, Meilan R**. **2013**. Constitutive expression of the Corngrass1
489 microRNA in poplar affects plant architecture and stem lignin content and composition. *Biomass*
490 *and Bioenergy* **54**: 312–321.
491 **Schwab R, Palatnik JF, Riester M, Schommer C, Schmid M, Weigel D**. **2005**. Specific
492 effects of microRNAs on the plant transcriptome. *Developmental Cell* **8**: 517–527.
493 **Scoffoni C, Sack L**. **2013**. Quantifying leaf vein traits. *Prometheus Wiki*.
494 **Stief A, Altmann S, Hoffmann K, Pant BD, Scheible W-R, Bäurle I**. **2014**. Arabidopsis

495 miR156 regulates tolerance to recurring environmental stress through SPL transcription factors.
496 *The Plant Cell* **26**: 1792–1807.
497 **Taylor G**. **2002**. Populus: Arabidopsis for forestry. Do we need a model tree? *Annals of Botany*
498 **90**: 681–689.
499 **Telfer A, Bollman KM, Poethig RS**. **1997**. Phase change and the regulation of trichome
500 distribution in Arabidopsis thaliana. *Development* **124**: 645–654.
501 **Varkonyi-Gasic E, Wu R, Wood M, Walton EF, Hellens RP**. **2007**. Protocol: A highly
502 sensitive RT-PCR method for detection and quantification of microRNAs. *Plant Methods* **3**: 12.
503 **Walters GA, Bartholomew DP**. **1984**. Acacia Koa leaves and phyllodes: Gas exchange,
504 morphological, anatomical, and biochemical characteristics. *Botanical Gazette* **145**: 351–357.
505 **Wang J-W**. **2014**. Regulation of flowering time by the miR156-mediated age pathway. *Journal*
506 *of Experimental Botany* **65**: 4723–4730.
507 **Wang JW, Park MY, Wang LJ, Koo Y, Chen XY, Weigel D, Poethig RS**. **2011**. MiRNA
508 control of vegetative phase change in trees. *PLoS Genetics* **7**: e1002012.
509 **Wang H, Wang H**. **2015**. The miR156/SPL module, a regulatory hub and versatile toolbox,
510 gears up crops for enhanced agronomic traits. *Molecular Plant* **8**: 677–688.
511 **Williams WP, Davis FM, Buckley PM, Hedin PA, Baker GT, Luthe DS**. **1998**. Factors
512 associated with resistance to fall Armyworm (Lepidoptera: Noctuidae) and southwestern Corn
513 Borer (Lepidoptera: Crambidae) in corn at different vegetative stages. *Journal of Economic*
514 *Entomology* **91**: 1471–1480.
515 **Xie K, Wu C, Xiong L**. **2006**. Genomic organization, differential expression, and interaction of
516 SQUAMOSA Promoter-Binding-Like Transcription Factors and microRNA156 in Rice. *Plant*
517 *Physiology* **142**: 280–293.
518 **Xu M, Hu T, Zhao J, Park M-Y, Earley KW, Wu G, Yang L, Poethig RS**. **2016**.
519 Developmental functions of miR156-regulated SQUAMOSA PROMOTER BINDING
520 PROTEIN-LIKE (SPL) genes in arabidopsis thaliana. *PLOS Genetics* **12**: e1006263.
521 **Zhang X, Zou Z, Zhang J, Zhang Y, Han Q, Hu T, Xu X, Liu H, Li H, Ye Z**. **2011**. Over-
522 expression of sly-miR156a in tomato results in multiple vegetative and reproductive trait
523 alterations and partial phenocopy of the *sft* mutant. *FEBS Letters* **585**: 435–439.
524 **Zheng Q-L, Liu J, Goff BM, Dinkins RD, Zhu H**. **2016**. Genetic manipulation of miR156 for
525 improvement of biomass production and forage quality in Red Clover. *Crop Science* **56**.

526 **Zotz G, Wilhelm K, Becker A**. **2011**. Heteroblasty-a review. *Botanical Review* **77**: 109–151.

527

528

529 **Figure 1.** miR156/7 relative abundance in *Populus tremula x alba* leaf primordia grown from
530 seed (A) or in transgenic and wildtype plants of the 717-1B4 background grown from tissue
531 culture (B). miR156/7 abundance relative to the average of 4 replicates from seed grown leaves 1
532 & 2. Data presented as individual biological replicates depicted by grey open circles and a mean
533 best fit line in black (A) or as means ± s.e.m (n = 3) with 717 wildtype data depicted by purple
534 circles, miR156a over-expressor lines depicted by blue squares and MIM156 lines depicted by
535 red triangles. Representative leaf shape for leaves 1-17, 20 and 30 from plants grown from seed
536 (C).
537
538 **Figure 2.** Representative plants from the wild-type 717-1B4, miR156a over-expressor line 40
539 and MIM156 line 84 two months following transplant from tissue culture. Representative leaf
540 shape for leaves 10, 15, 20 and 25 in the 717-1B4 and transgenic poplar plants from tissue
541 culture.
542
543 **Figure 3.** Number of leaves initiated by *P. tremula x alba* grown from seed (A) and the 717-1B4
544 wildtype and four transgenic lines from tissue culture (n = 3-6) (B). Internode distance between
545 nodes 10-20 (n = 6) (C), and number of branches of > 1cm in length between nodes 1 and 25
546 after 230 days of growth (n = 6) (D) in the 717-1B4 and four transgenic lines. Symbols and
547 colors are the same as figure 1 with seed grown data presented as individual biological replicates
548 and 717-1B4 lines as means ± s.e.m. Data in panel A show a second-degree polynomial
549 relationship with $p < 0.0001$ and R^2=0.92 and a two-way *ANOVA* for panel B found $p < 0.0001$
550 for genotype and days after transplant but no significance for an interaction between effects.
551 One-way *ANOVA* for panels C and D found $p < 0.0001$ with the results of a *Student's T* between
552 WT and mutants represented by * $p < 0.05$, ** $p < 0.01$, and *** $p < 0.001$.
553
554 **Figure 4.** Leaf length:width (L:W) ratio, leaf area, specific leaf area (SLA), abaxial trichome
555 density, adaxial stomatal density, abaxial stomatal density, and adaxial epidermal cell area of
556 seed grown poplar (A, C, E, G, I, K, M) and the 717-1B4 and transgenic lines (B, D, F, H, J, L,
557 N). Symbols and colors are the same as figure 1 with seed grown data presented as individual
558 biological replicates and 717-1B4 lines as means ± s.e.m (n = 5-11). Data in panels A, C, E, G
559 and M show a second-degree polynomial relationship with p <0.0001 and R^2 values of 0.17, 0.6,

560 0.32, 0.56 and 0.85 respectively. Data in panels I and K show a linear relationship with p
561 <0.0001 and R^2 values of 0.58 and 0.46 respectively. Two-way *ANOVA*s with leaf position and
562 genotype as the effects for data in panels B, D, F, H, L and N found $p<0.001$ for both leaf
563 position and genotype. In panel J, $p<0.001$ for genotype but N.S. for leaf position. For the
564 interaction between genotype and leaf position, $p<0.05$ for data in panels B, F, H, and L and
565 N.S. for panels D, J, and N.
566
567 **Figure 5.** Total leaf vein density (A) and the number of vein endings (B) in the 717-1B4 and
568 transgenic plants. Symbols and colors are the same as figure 1 with data presented as means ±
569 s.e.m (n = 5-6). A two-way *ANOVA* with leaf position and genotype as the effects found p
570 <0.0001 for both effects and the interaction for data in panels A and B. Representative samples
571 of leaves cleared and stained with safranin-O to visualized vein density and architecture in leaves
572 10 and 25 of 717-1B4 and transgenic poplar lines (C).
573
574 **Figure 6.** Petiole length:width ratio from cross sections made within 1 cm of leaf attachment in
575 seed grown (A) and 717-1B4 and transgenic poplar (B). Symbols and colors are the same as
576 figure 1 with seed grown data presented as individual biological replicates and 717-1B4 lines as
577 means ± s.e.m (n = 7-12). Data from panel A show a second-degree polynomial relationship with
578 $p<0.0001$ and $R^2 = 0.62$. For panel B, a two-way *ANOVA* with leaf position and genotype as the
579 effects found $p< 0.0001$ for leaf position and genotype and $p=0.01$ for the interaction.
580 Representative samples of petiole cross sections stained with safranin-O from leaves 10, 15, 20
581 and 25 of the 717-1B4 and four transgenic lines (C).
582
583 **Figure 7.** Diagram showing the path length and horizontal span measurements of leaf fluttering
584 of a WT 717-1B4 adult leaf at node 25, juvenile leaf at node 10, and a miR156 over-expressor
585 line 40 juvenile leaf at node 25 (A). Quantification of leaf fluttering through total path length
586 over a 1 second period (B) and maximum horizontal span of the tip of the leaf (C) and their
587 relationship with petiole length:width ratio. WT 717-1B4 data is depicted by circles,
588 miR156aOX line 40 by squares and MIM156 line 84 by open triangles. Leaf developmental
589 stage is noted by color with adult leaves (node 25) in red, juvenile (node 10) in dark blue and
590 juvenilized (node 25) from miR156 overexpression in light blue. Linear fit for panel A) path

length = -0.34288 + 0.544(petiole L:W ratio) and B) horizontal span = -0.0852 + 0.0939(petiole L:W ratio).

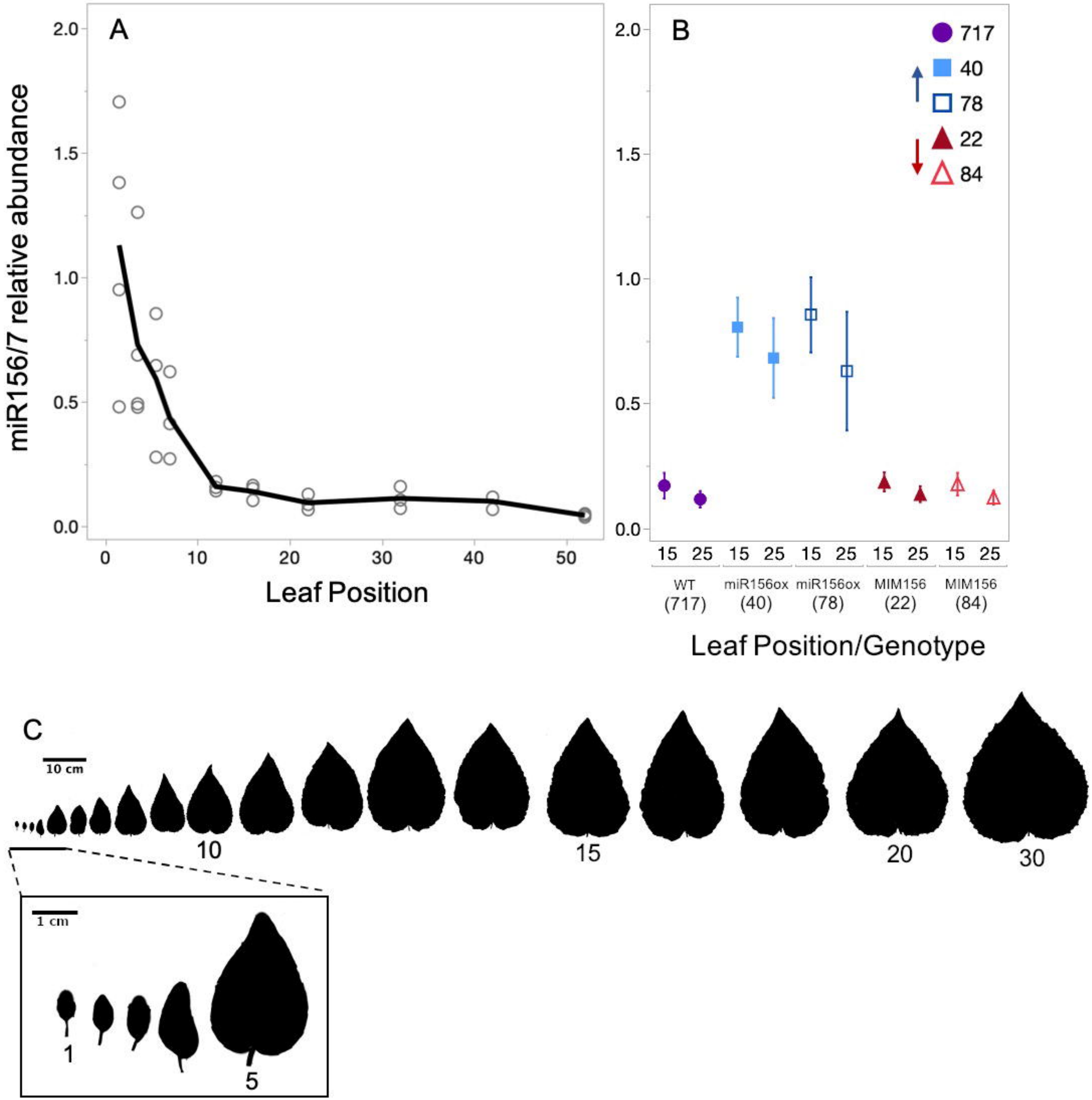
A
miR156/7 relative abundance
2.0
1.5
1.0
0.5
0.0
0
10
20
30
40
50
Leaf Position
B
717
40
78
22
84
15 25 15 25 15 25 15 25 15 25
WT (717)
miR156ox (40)
miR156ox (78)
MIM156 (22)
MIM156 (84)
Leaf Position/Genotype
C
10 cm
10
15
20
30
1 cm
1
5

WT 717-1B4
miR156a ox
MIM156

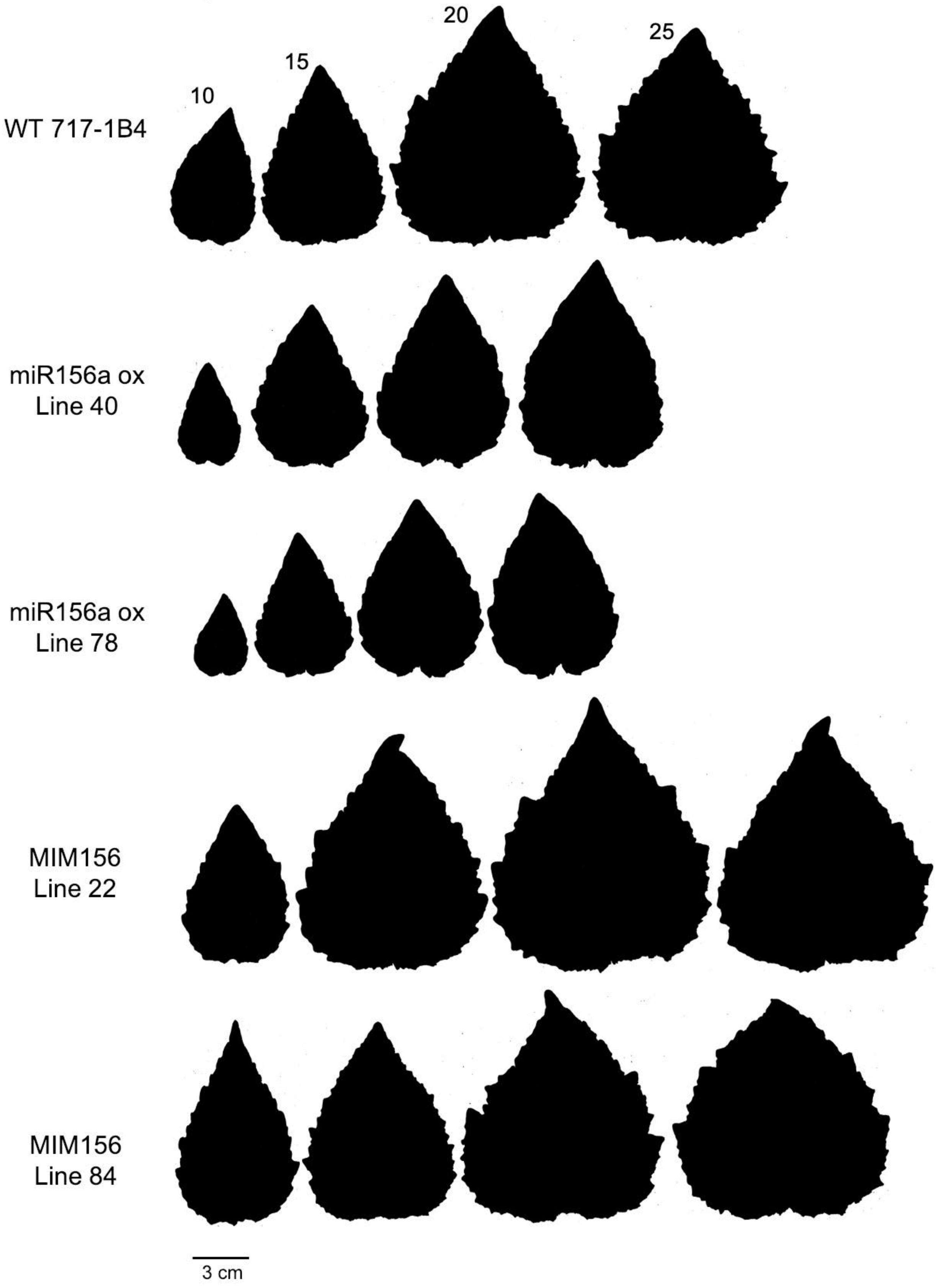
10
15
20
25
WT 717-1B4
miR156a ox
Line 40
miR156a ox
Line 78
MIM156
Line 22
MIM156
Line 84
3 cm

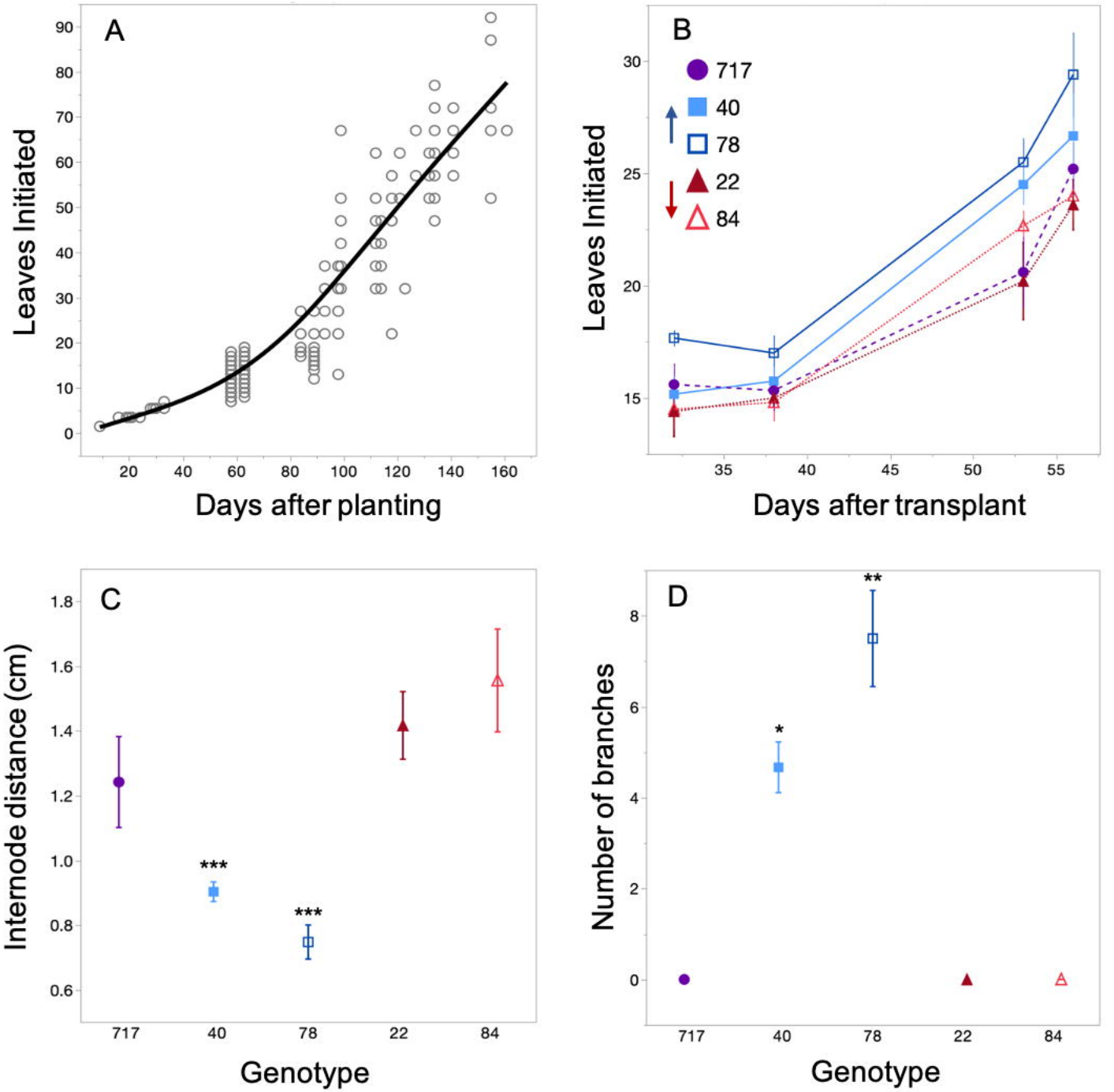
A
Leaves Initiated
Days after planting
B
717
40
78
22
84
Leaves Initiated
Days after transplant
C
Internode distance (cm)
***
***
717
40
78
22
84
Genotype
D
Number of branches
*
**
717
40
78
22
84
Genotype

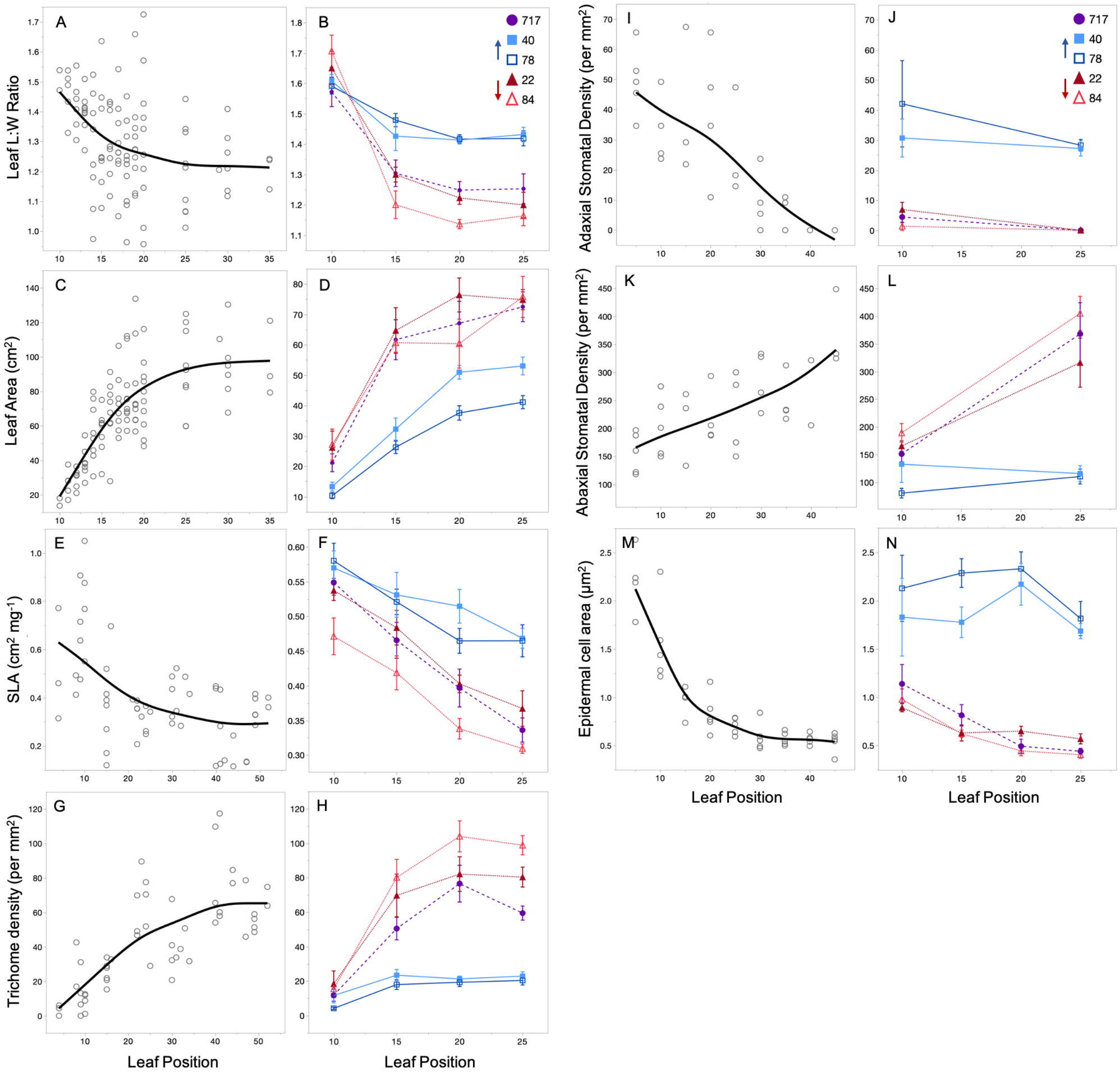
A
B
C
D
E
F
G
H
I
J
K
L
M
N
717
40
78
22
84
Leaf L:W Ratio
Leaf Area (cm²)
SLA (cm² mg⁻¹)
Trichome density (per mm²)
Adaxial Stomatal Density (per mm²)
Abaxial Stomatal Density (per mm²)
Epidermal cell area (µm²)
Leaf Position
Leaf Position
Leaf Position
Leaf Position

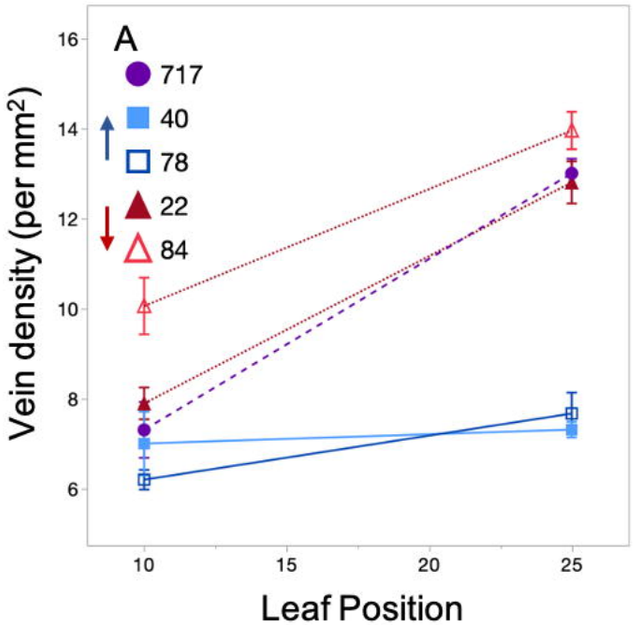
A
717
40
78
22
84
Vein density (per mm²)
Leaf Position

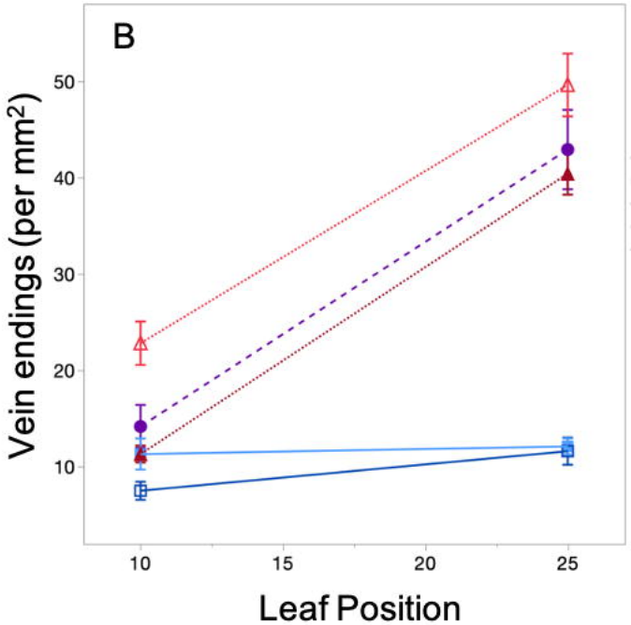
B
Vein endings (per mm²)
Leaf Position

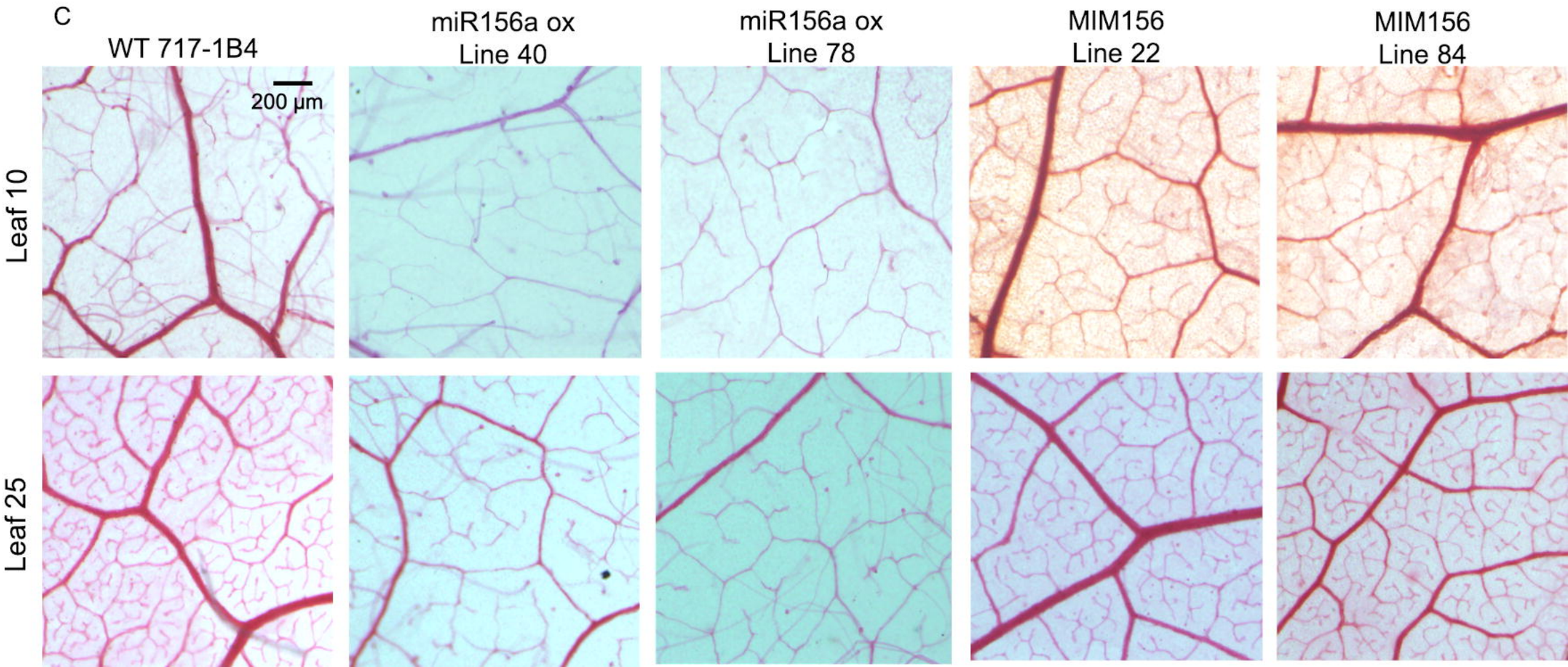
C
WT 717-1B4
miR156a ox
Line 40
miR156a ox
Line 78
MIM156
Line 22
MIM156
Line 84
200 µm
Leaf 10
Leaf 25

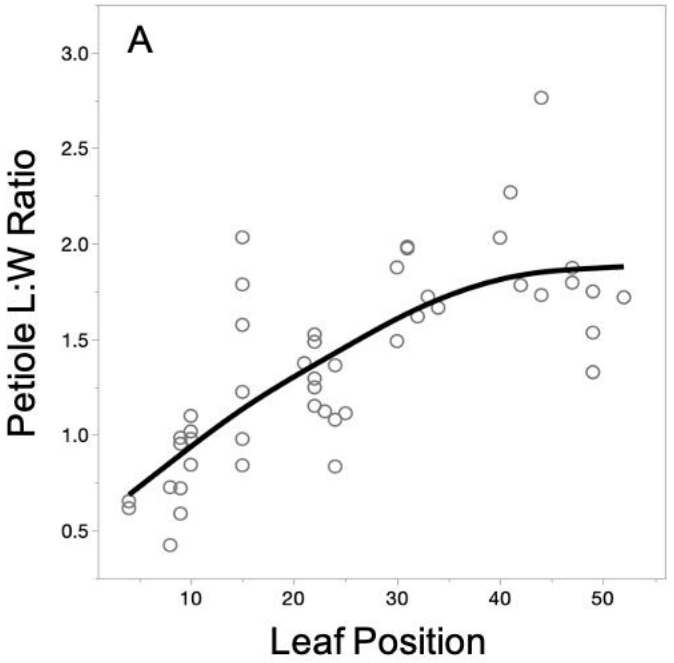
A
Petiole L:W Ratio
Leaf Position
3.0
2.5
2.0
1.5
1.0
0.5
10
20
30
40
50

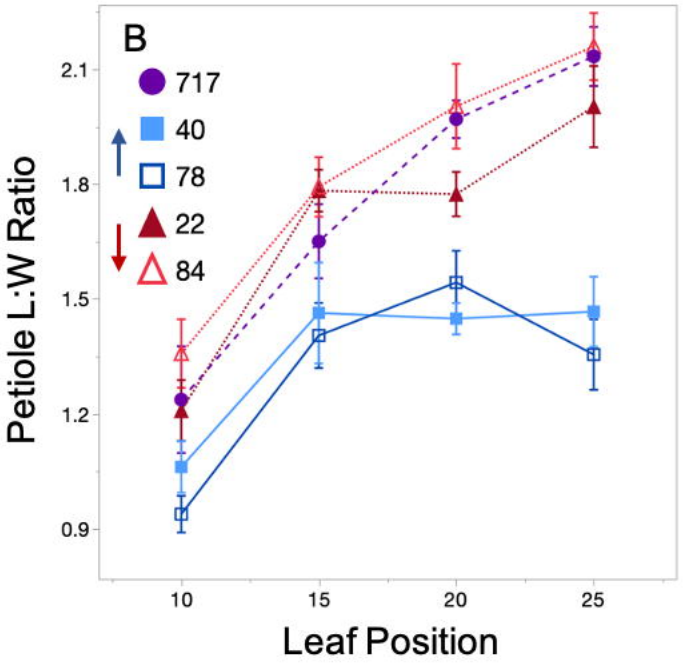
B
717
40
78
22
84
Petiole L:W Ratio
Leaf Position
2.1
1.8
1.5
1.2
0.9
10
15
20
25

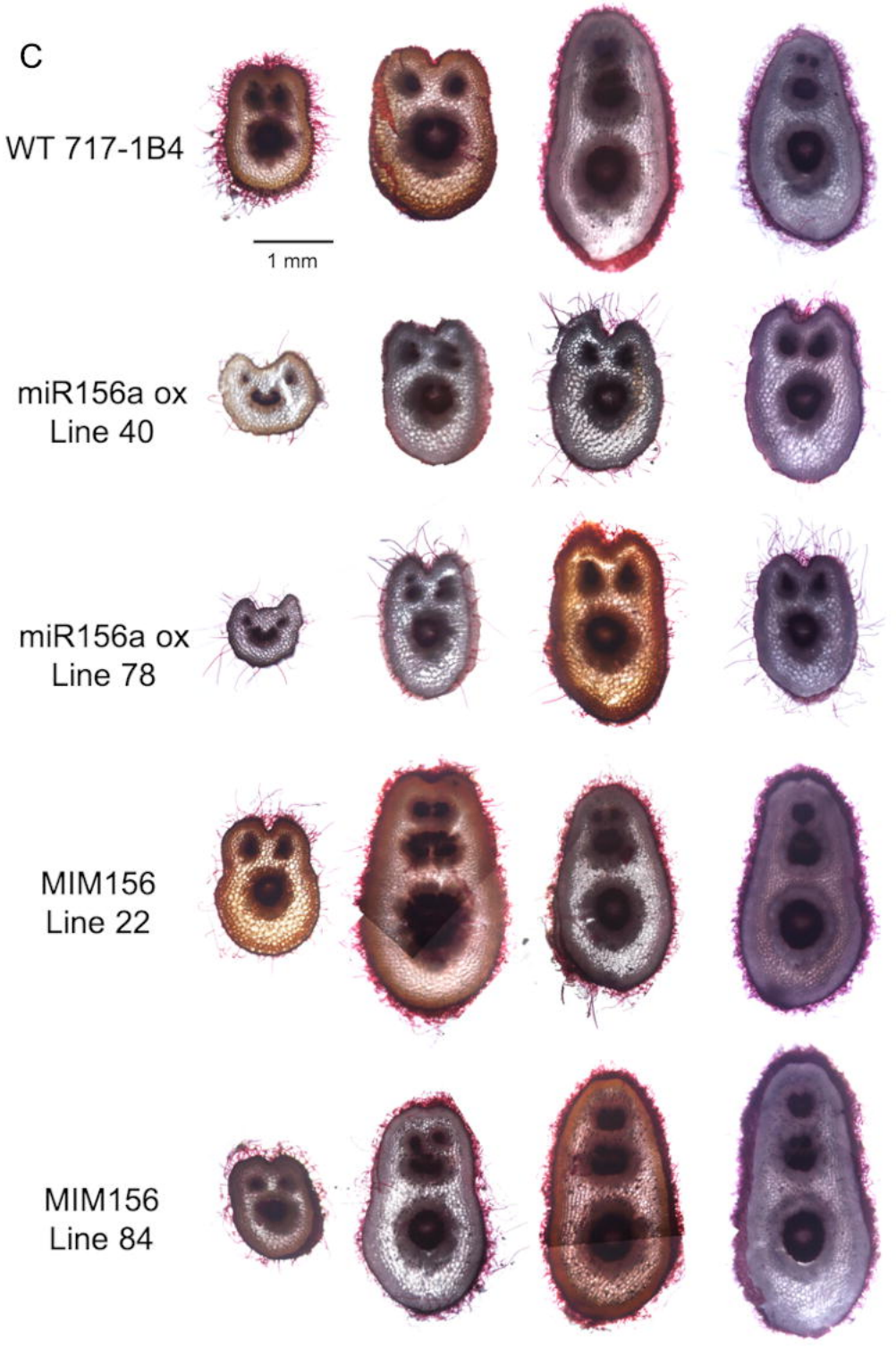
C
WT 717-1B4
1 mm
miR156a ox
Line 40
miR156a ox
Line 78
MIM156
Line 22
MIM156
Line 84

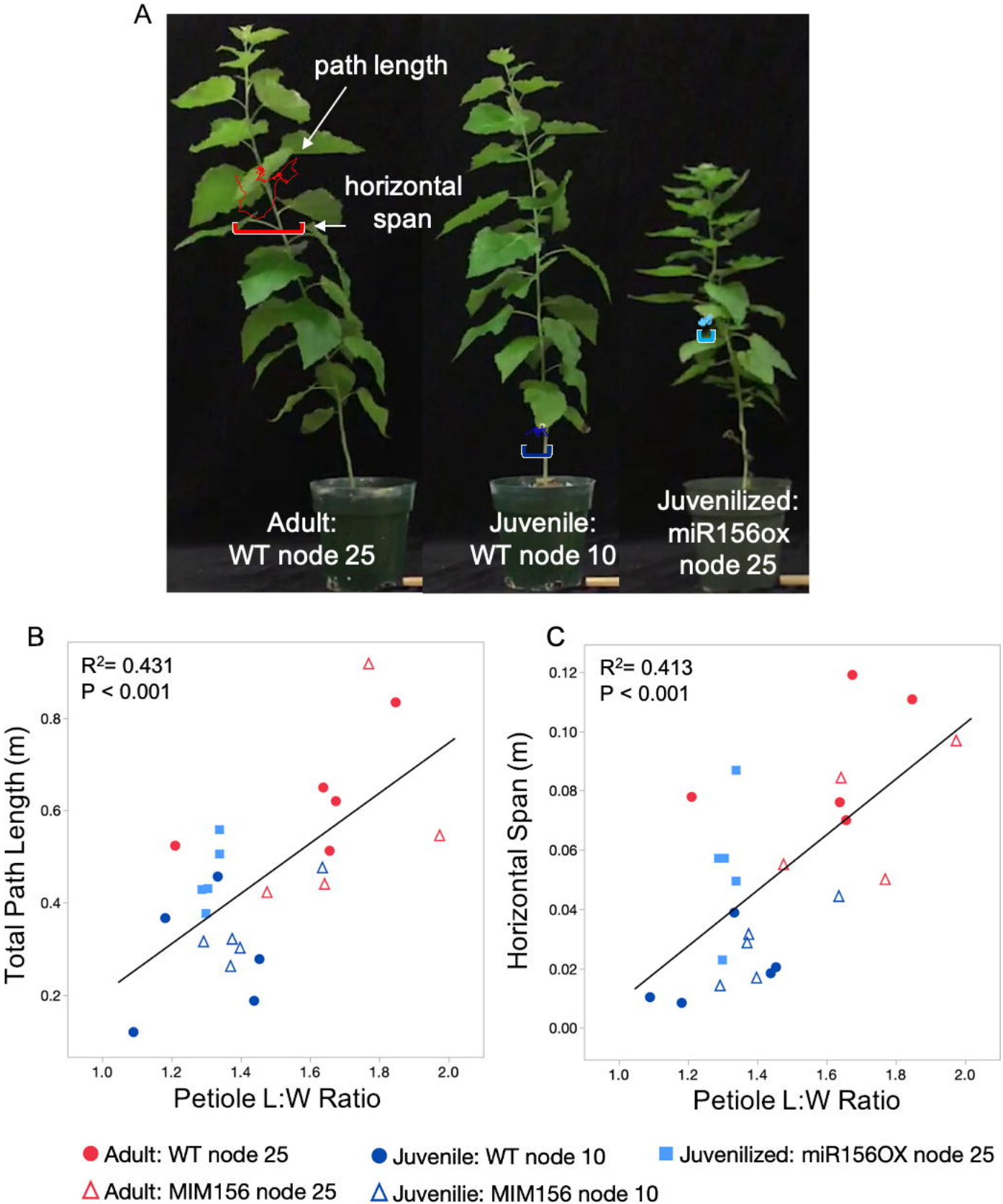
A
path length
horizontal span
Adult: WT node 25
Juvenile: WT node 10
Juvenilized: miR156ox node 25
B
R2= 0.431
P < 0.001
Total Path Length (m)
Petiole L:W Ratio
C
R2= 0.413
P < 0.001
Horizontal Span (m)
Petiole L:W Ratio
Adult: WT node 25
Juvenile: WT node 10
Juvenilized: miR156OX node 25
Adult: MIM156 node 25
Juvenilie: MIM156 node 10